

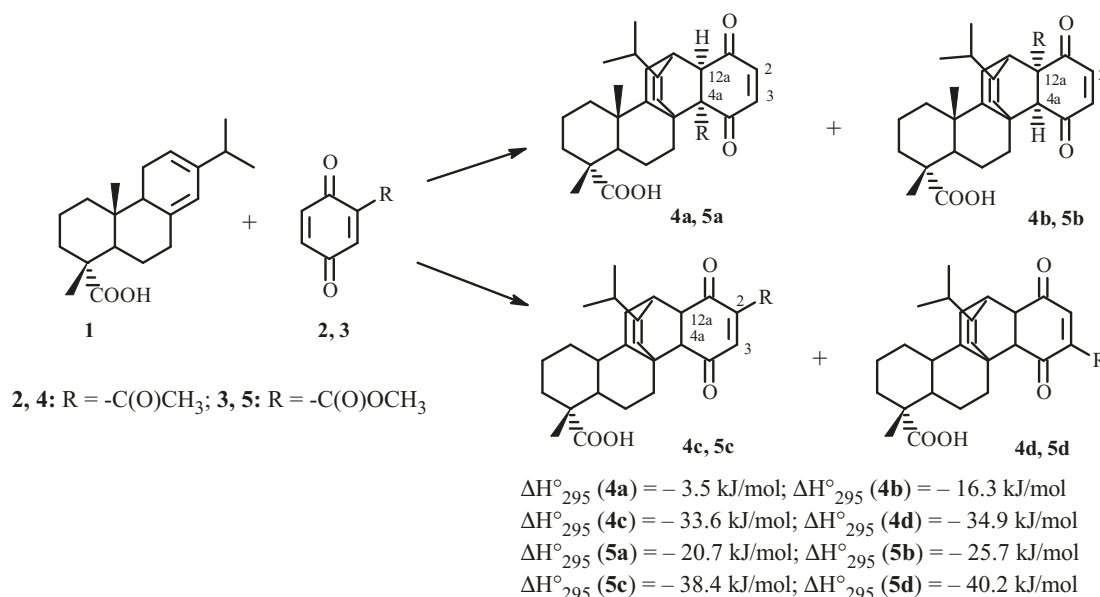
## EXPERIMENTAL AND THEORETICAL JUSTIFICATION FOR THE REGIOSPECIFIC CYCLOADDITION OF LEVOPIMARIC ACID TO 2-ACETYL- OR 2-(METHOXYCARBONYL)-1,4-BENZOQUINONE

G. F. Vafina,\* S. S. Borisevich, A. R. Uzbekov,  
A. I. Poptsov, L. V. Spirikhin, and S. L. Khursan

New 4a-quinopimaric acid derivatives were synthesized via a Diels–Alder reaction of levopimaric acid with 2-acetyl- or 2-(methoxycarbonyl)-1,4-benzoquinone and were characterized using elemental analysis and NMR spectroscopy. Thermodynamic and activation parameters of the Diels–Alder reactions of levopimaric acid and a model diene (7-isopropyl-1,2,3,4,4a,5-hexahydronaphthalene) with 2-acetyl- or 2-(methoxycarbonyl)-1,4-benzoquinone were calculated by density-functional theory in order to explain the observed regioselective cycloaddition.

**Keywords:** diene synthesis, quinopimaric acid, density-functional theory.

The reaction of levopimaric acid with quinones is one of the most interesting diene syntheses, which are promising methods for synthesizing polycyclic compounds. This is due to the fact that many quinone derivatives of diterpenic acids have recently exhibited biological activity including antitumor and antiviral [1]. Several levopimaric-acid derivatives (dihydroquinopimaric acid, adducts with 2-acetylaminquinone, sulfonylnaphthoquinone, and 3-hexylthio-2-thiolen-4-one-1,1-dioxide) acted as anti-inflammatory agents [1]. The diene-synthesis reaction of levopimaric acid with 2-acetyl- or 2-methoxycarbonyl-1,4-benzoquinone is interesting with respect to the potential discovery of optically active compounds with biological activity.



Ufa Institute of Chemistry, Russian Academy of Sciences, 450054, Ufa, Prosp. Oktyabrya, 71, e-mail: vafina@anrb.ru.  
Translated from *Khimiya Prirodnykh Soedinenii*, No. 6, November–December, 2015, pp. 964–969. Original article submitted April 10, 2015.

In continuation of studies on the synthesis of new quinopimaric-acid derivatives [2], we studied the Diels–Alder reaction of levopimaric acid (**1**) contained (~30%) in pine tar with 2-acetyl- (**2**) and 2-(methoxycarbonyl)-1,4-benzoquinone (**3**). The reaction occurred stereo- and regioselectively during seven days to give only regioisomers **4a** and **5a** in 99 and 73% yields, respectively.

The position of the R substituent was determined using PMR and NMR correlation spectra of **4a**. Thus, the PMR spectrum showed two doublets at  $\delta$  5.97 and 6.03 ppm with SSCC 10.2 Hz that were consistent with protons of a 2(3) double bond. The proton of the other double bond resonated as a singlet at  $\delta$  5.33 ppm. A singlet at  $\delta$  71.82 ppm in the  $^{13}\text{C}$  NMR spectrum belonged to C-4a and indicated that the acetyl was located at this position. The proton with chemical shift (CS) 3.25 ppm in the HSQC spectrum correlated with C-12a ( $\delta$  56.40 ppm). The proton with CS 2.79 ppm gave a cross peak with C-12 ( $\delta$  40.84 ppm). Proton H-12a ( $\delta$  3.25 ppm) gave cross peaks with C-4a ( $\delta$  71.82 ppm), C-4b ( $\delta$  46.72 ppm), C-11 ( $\delta$  30.13 ppm), C-12 ( $\delta$  40.84 ppm), and C-13 ( $\delta$  148.52 ppm) and with the three ketones C-1, C-4, and  $\text{C}=\text{O}$ . The  $^1\text{H}$ – $^1\text{H}$  COSY spectrum of H-12a indicated correlations with H-12 and H-11ax although the SSCC between them was  $<1$  Hz. The NOESY spectrum showed correlations of the acetyl methyl protons with H-10b and H-12a. This confirmed that it had the  $\alpha$ -position and that rings D and E were *cis*-fused. The same scenario was observed for **5a**.

Thus, addition of 2-substituted-1,4-benzoquinones **2** or **3** to levopimaric acid (**1**) formed a single adduct in which the substituent (acetyl or methoxycarbonyl) was located in the 4a-position at the ring fusion site. This contrasted with all previously synthesized quinopimaric-acid derivatives, in which the substituents were terminal (on the side of the C-2=C-3 double bond) [2]. On one hand, this agreed with previous results [3–5] for dienophiles **2** and **3** in diene syntheses. On the other, a diene synthesis of *in-situ*-generated 2-acetylbenzoquinone with 1-methyl-1,3-butadiene in THF–TFA and  $\text{Pb}_3\text{O}_4$  proceeded anomalously and formed a product in which the acetyl was located on the terminal C-2=C-3 double bond [6]. The Diels–Alder reaction of levopimaric acid with dienophiles **2** and **3** was investigated using density-functional theory in order to obtain additional information regarding the dominant steric effects for this system.

NMR spectral data showed unambiguously that the reaction of levopimaric acid with 2-acetyl- and 2-(methoxycarbonyl)-1,4-benzoquinones (**2** and **3**) formed only the *endo*-adducts. This phenomenon is well-known in the literature [7] and is called the Alders *endo*-effect. Therefore, we did not analyze the possible *exo*-directed cycloaddition. It was obvious considering this model limitation that the addition of **2** and **3** to **1** could form four *endo*-oriented regioisomers **4a–d** (**5a–d**), the structures of which depended on the positioning of the second reagent relative to the acid reactive center.

The studied reaction was exothermic for both benzoquinones. The quantity  $\Delta_f H_{295}^\circ$  was greatest for the reaction leading to adducts **4a** and **5a**. The enthalpies of formation of regioisomers **4a–d** and **5a–d** [B3LYP/6-311+G(d,p)] were calculated considering solvation ( $\text{CH}_2\text{Cl}_2$ ) at 295 K. The result indicated that the formation of these compounds was least probable with respect to thermodynamic stability. However, regioisomers **4a** and **5a** were the only reaction products according to NMR studies (see above). Therefore, the preferential formation of **4a** (**5a**) was due to kinetic factors, i.e., the faster formation of these isomers due to differences in the activation energies for forming regioisomers **4a–d** (**5a–d**). This hypothesis was checked by locating all four possible transition states (TS) for the [4+2]-cycloaddition reaction using the reactions of **2** and **3** with the model diene 7-isopropyl-1,2,3,4,4a,5-hexahydronaphthalene (**6**) as examples. Diene **6** was selected as a simplified analog of **1** in order to conserve computing time and preserved all structural features of the levopimaric-acid reaction centers. The numbering for model products **7a–d** (**8a–d**) is the same as for adducts **4a–d** (**5a–d**).

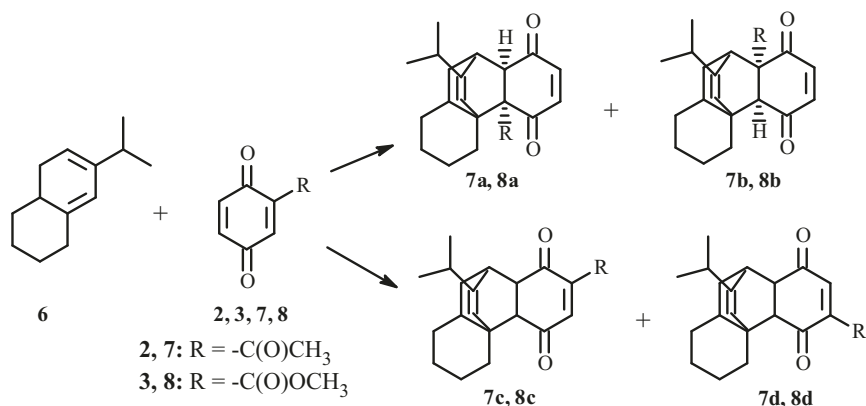


TABLE 1. Enthalpies of Reaction ( $\Delta_r H^\circ$ ) and Activation ( $\Delta H^\ddagger$ ) at the B3LYP/6-311+G(d,p) Level for the Reaction of **6** with 2-Acetyl- and 2-(Methoxycarbonyl)-1,4-benzoquinones

Reaction	$\Delta H^\ddagger$ , kJ/mol	$\Delta_r H^\circ_{295}$ , kJ/mol	Reaction	$\Delta H^\ddagger$ , kJ/mol	$\Delta_r H^\circ_{295}$ , kJ/mol
<b>6</b> + <b>2</b> → <b>7a</b>	<b>70.6</b>	<b>-19.4</b>	<b>6</b> + <b>3</b> → <b>8a</b>	<b>75.9</b>	<b>-35.9</b>
<b>6</b> + <b>2</b> → <b>7b</b>	88.8	-30.3	<b>6</b> + <b>3</b> → <b>8b</b>	93.1	-39.2
<b>6</b> + <b>2</b> → <b>7c</b>	85.3	-47.1	<b>6</b> + <b>3</b> → <b>8c</b>	106.6	-49.4
<b>6</b> + <b>2</b> → <b>7d</b>	84.6	-48.3	<b>6</b> + <b>3</b> → <b>8d</b>	103.8	-53.1

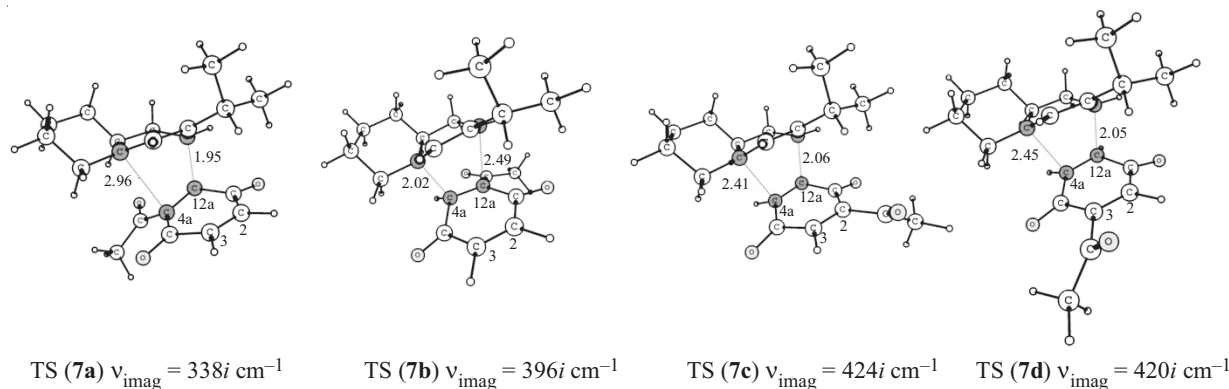


Fig. 1. Transition states (TS) for the reaction of 7-isopropyl-1,2,3,4,4a,5-hexahydronaphthalene with 2-acetyl-1,4-benzoquinone at the B3LYP/6-311+G(d,p) level; bond lengths are given in Å; the value of the only imaginary frequency  $\nu_{\text{imag}}$  is given for each TS.

The Diels–Alder reaction of **6** with **2** and **3** formed cyclic TS with similar geometric parameters. The presence of a single imaginary frequency in the calculated TS vibrational spectrum confirmed that they were valid. Figure 1 shows the structures of the activated complexes of the four possible adducts from the Diels–Alder reaction of **6** with **2** as examples.

The activated complexes and products from the reaction of **6** with **2** and **3** were localized on the system potential-energy surface. This allowed the activation energy  $\Delta H^\ddagger$  and enthalpies of reaction  $\Delta_r H^\circ$  to be calculated for the corresponding directions with consideration of solvation ( $\text{CH}_2\text{Cl}_2$ ) at 295 K and 1 atm. Table 1 lists the results.

The fact that the thermodynamic stabilities of **7a–d** (**8a–d**) followed the same order as those of **4a–d** (**5a–d**) confirmed that the simplified model was valid (Table 1). Model product **7a** (**8a**) was thermodynamically the least stable. Therefore, its preferential formation was explained by other factors. In fact, our calculations showed that the barrier height of the heat of formation  $\Delta H^\ddagger$  for **7a** (**8a**) was the lowest. The difference in the TS energies was 15 kJ/mol and greater. This indicated that the other isomers formed negligibly slowly compared to **7a** (**8a**).

Thus, DFT calculations confirmed theoretically that **4a** and **5a** were formed exclusively in our experiments. Let us discuss briefly the effects of the cycloaddition regioselectivity using our calculations.

Frontier molecular orbitals are often and successfully used to explain the course of Diels–Alder reactions. An orbital diagram (Fig. 2) that was constructed using our results showed as expected that the course of the reaction of **1** (**6**) with **2** (**3**) was controlled by interaction of the highest occupied molecular orbital (HOMO) of the diene with the lowest unoccupied molecular orbital (LUMO) of the mono-substituted benzoquinone. Because the latter displays electrophilic properties, the C=C bond with elevated electrophilicity due to the electron-accepting effect of the –COMe (–COOMe) substituent will be the more reactive of the two centers in **2** (**3**). Figure 2 shows that more strongly accepting substituents gave lower LUMO energies and lower energy splitting for the HOMO–LUMO pair. The cycloaddition was favored as the frontier orbitals drew closer. Therefore, the acetyl- or (methoxycarbonyl)-substituted C=C bond in **2** or **3** was more reactive than the unsubstituted one despite the possible steric hindrance. Furthermore, the order of reactivities of the mono-substituted benzoquinones from DFT calculations agreed fully with the experimental sequence for diene syntheses of benzoquinones [8].

The regioselectivity of the reaction was also apparent in the positioning of the acetyl or methoxycarbonyl substituent exclusively in the 4a-position of quinopimaric acid. Our DFT calculations confirmed the conclusion based on NMR studies and provided a theoretical explanation of the observed effect.

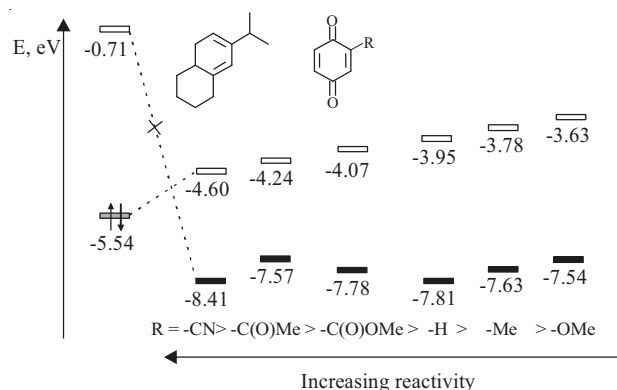
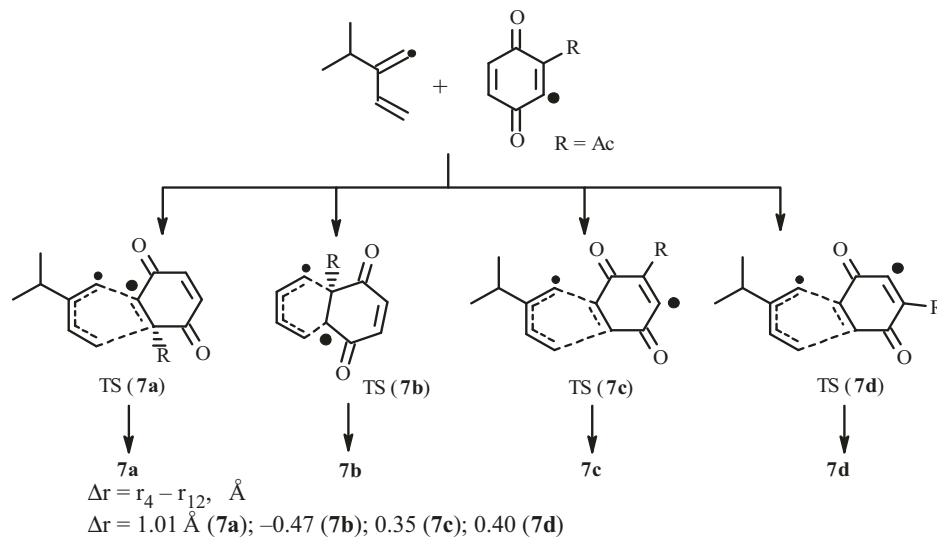


Fig. 2. Frontier orbital energies [B3LYP/6-311+G(d,p)] for diene **6** and several substituted 1,4-benzoquinones.

The studied transformations occurred through the two-center addition mechanism typical of Diels–Alder reactions [7]. However, the C–C bonds in the TS were not formed synchronously (Fig. 1). The nature of the asynchronicity and its scale, which was estimated as the difference of the resulting bond lengths, varied as a function of the acetyl position. Interatomic distance  $r_{12}$  in TS(7a), i.e.,  $r(\text{C}12\text{--C}12a)$ , was significantly shorter than  $r_4 = r(\text{C}4b\text{--C}4a)$  whereas the reverse relationship of bond lengths ( $r_4 < r_{12}$ ) was noted for TS(7b). The effect was less pronounced in the other two TS (Fig. 1) although  $r_4 > r_{12}$ .

The reaction of model diene **6** (and also **1**) is a classical instance of the reaction of reagents containing substituents with opposing electronic effects. The weakly electron-donating isopropyl radical in **6** affects the molecular wave function so that the AO coefficient of the neighboring C atom (marked by a dot in the diagram) in the MO LCAO expansion for the HOMO is increased. In a similar manner, the electron-accepting substituent in 2-acetyl-1,4-benzoquinone increases the AO coefficient on the distal C atom of the double bond in the expansion of the LUMO of the dienophile over the basis AO. This C atom is marked with a large dot in the diagram because the acetyl substituent displays strong accepting properties.



Only the substituted diene moiety of **6** is shown in the diagram for simplicity. The values  $\Delta r = r_4 - r_{12}$  are shown. The HOMO–LUMO overlap for forming the  $r_{12}$  bond is maximum in the TS corresponding to the major reaction adduct **7a**. As a result, the distance between C atoms marked with dots in the diagram will be much less than the length of C–C bonds formed in the other activated complexes. This is clearly illustrated by the quantum-chemical calculations (Fig. 1). The diagram explains correctly the TS asynchronicity in all instances. For example, if the acetyl substituent is located on the side of the terminal C=C double bond [TS(7c, 7d)], then the moderate asynchronicity of forming the C–C bonds in the TS is due only to the effect of the isopropyl substituent in **6**. The effectiveness of orbital overlap in the TS is reflected in the activation energy and explains the variation of  $\Delta H^\ddagger$  for the different courses of the cycloaddition (Table 1). Obviously, all electronic effects examined using 2-acetyl-1,4-benzoquinone as an example are valid for **3**.

Thus, the formation of only adducts **4a** and **5a** in the reaction of levopimaric acid with 2-acetyl- or 2-(methoxycarbonyl)-1,4-benzoquinones is explained primarily by the interaction of the reagent frontier orbitals. The substituents in both reagents affect their energy and composition. This interaction controls both the reaction energetics and its regioselectivity.

## EXPERIMENTAL

PMR and  $^{13}\text{C}$  NMR spectra were recorded in  $\text{CDCl}_3$  on a pulsed Bruker Avance-III spectrometer (500 MHz) at operating frequency 500.13 MHz for  $^1\text{H}$  and 125.47 MHz for  $^{13}\text{C}$ . Chemical shifts in PMR and  $^{13}\text{C}$  NMR spectra are given in ppm vs. solvent resonances. 2D correlation spectra were recorded using the standard instrument library of pulse sequences. IR spectra of thin layers were taken on a Shimadzu instrument. Elemental analysis was performed on a Euro EA 3000 analyzer. Melting points were uncorrected and were measured on a Boetius apparatus. NMR, mass, and IR spectra were recorded on equipment at the Khimiya CCU, UIC, RAS. Elemental analyses of all synthesized compounds agreed with those calculated.

The course of reactions was monitored by TLC on Sorbfil PTSKh-AF-A plates. Compounds were detected by spraying with  $\text{H}_2\text{SO}_4$  solution (5%) followed by heating to 100–120°C. The eluent was  $\text{CHCl}_3$ -MeOH (50:1, 10:1, 5:1). Flash chromatography was carried out over standard silica gel 60 (0.04–0.063 mm, 230–400 mesh) (Macherey–Nagel, Germany).

2-Acetyl-1,4-benzoquinone was prepared via oxidation of 2,5-dihydroxyacetophenone by  $\text{Ag}_2\text{O}$  [9]. 2-(Methoxycarbonyl)-1,4-benzoquinone was prepared in two steps from 2,5-dihydroxybenzoic acid (first, methylation by diazomethane; second, oxidation by  $\text{Ag}_2\text{O}$  [9]). Physicochemical data for the synthesized quinones agreed with those in the literature. We used *Pinus sylvestris* pine tar containing ~30% levopimaric acid that was collected in spring 2012 near Nizhni Novgorod. The levopimaric acid content in the pine tar was determined using GC and the ratio of methyl esters of total resinous acids that were produced by methylating pine tar with an excess of diazomethane. The product yields were calculated per starting quinone.

**Diene Synthesis Method.** Pine tar (5 g) in  $\text{CH}_2\text{Cl}_2$  (50 mL) was treated with the appropriate quinone (0.05 mol) in hexane (2.5 mL). The reaction mixture was stored in the dark at room temperature for 7 d. The solvent was vacuum distilled (water aspirator). The residue was crystallized from petroleum ether (40–70°C).

**(7R,10aR,12aS,4aS)-4a-Acetyl-13-isopropyl-7,10a-dimethyl-1,4-dioxo-4,4a,5,6,6a,7,8,9,10,10a,10b,11,12,12a-tetradecahydro-1H-4b,12-ethenochrysen-7-carboxylic Acid (4a).**  $\text{C}_{28}\text{H}_{36}\text{O}_5$ , quantitative yield. Acid **4a** was isolated pure as a bright-yellow powder by crystallization from MeOH–hexane, mp 75–78°C (MeOH–hexane),  $[\alpha]_{\text{D}}^{20} -129^\circ$  (*c* 1.2,  $\text{CHCl}_3$ ). IR spectrum ( $\nu$ ,  $\text{cm}^{-1}$ ): 3177, 1733, 1723, 1667, 1616, 1464, 1377, 1363, 1277, 1189, 1028.  $^1\text{H}$  NMR spectrum ( $\text{C}_6\text{D}_6$ ,  $\delta$ , ppm, J/Hz): 0.55 (3H, s, Me-7), 0.73–0.75 (1H, m,  $\text{H}_{\text{eq}}-10$ ), 0.76 (3H, d, *J* = 7.1, Me), 0.78 (3H, d, *J* = 7.1, Me), 0.92–0.97 (1H, m,  $\text{H}_{\text{eq}}-11$ ), 1.06 (1H, d, *J* = 12.6,  $\text{H}_{\text{ax}}-10$ ), 1.16 (3H, s, Me-10a), 1.21–1.32 (3H, m,  $\text{H}_{\text{eq}}-9$ ,  $\text{H}_{\text{eq}}-6$ ,  $\text{H}_{\text{ax}}-9$ ), 1.39–1.45 (1H, m,  $\text{H}_{\text{ax}}-6$ ), 1.49 (1H, d, *J* = 13.3,  $\text{H}_{\text{eq}}-8$ ), 1.55–1.62 (1H, m,  $\text{H}_{\text{ax}}-11$ ), 1.70 (3H, s, MeCO), 1.75 (1H, dd, *J* = 13.3, 4.0,  $\text{H}_{\text{ax}}-8$ ), 1.86 (1H, septd,  $^3\text{J} = 7.1$ ,  $^4\text{J} = 1.7$ , H-15), 2.00 (1H, dd, *J* = 10.5, 1.6, H-10b), 2.09 (1H, td, *J* = 13.6, 4.9, 4.9,  $\text{H}_{\text{eq}}-5$ ), 2.37 (1H, dd, *J* = 9.6, 5.6, H-6a), 2.50 (1H, dt, *J* = 13.6, 3.1,  $\text{H}_{\text{ax}}-5$ ), 2.79 (1H, t, *J* = 0.7, H-12), 3.25 (1H, s, H-12a), 5.25 (1H, s, H-14), 5.98 (1H, d,  $J_{2-3} = 10.2$ , H-2), 6.03 (1H, d,  $J_{3-2} = 10.2$ , H-3).  $^{13}\text{C}$  NMR spectrum ( $\text{C}_6\text{D}_6$ ,  $\delta$ , ppm): 15.74 (q, Me), 16.57 (q, Me), 16.91 (t, C-9), 19.75 (q, Me), 20.06 (q, Me), 22.29 (t, C-6), 30.12 (q, Me), 30.13 (t, C-11), 32.02 (t, C-5), 32.57 (d, C-15), 36.53 (t, C-8), 37.76 (t, C-10), 37.87 (s, C-10a), 40.84 (d, C-12), 46.05 (d, C-6a), 46.72 (s, C-4b), 47.49 (s, C-7), 47.98 (d, C-10b), 56.40 (d, C-12a), 71.82 (s, C-4a), 127.46 (d, C-14), 138.74 (d, C-3), 143.67 (d, C-2), 148.52 (s, C-13), 185.58 (s, COO), 196.81 (s, C-4=O), 198.16 (s, COMe), 202.14 (s, C-1=O).

**(7R,10aR,12aS,4aS)-13-Isopropyl-4a-(methoxycarbonyl)-7,10a-dimethyl-1,4-dioxo-4,4a,5,6,6a,7,8,9,10,10a,10b,11,12,12a-tetradecahydro-1H-4b,12-ethenochrysen-7-carboxylic Acid (5a).**  $\text{C}_{28}\text{H}_{36}\text{O}_6$ , 73% yield. Acid **5a** was isolated pure as a bright-yellow powder by crystallization from  $\text{Et}_2\text{O}$ –hexane, mp 58–60°C,  $[\alpha]_{\text{D}}^{20} -53^\circ$  (*c* 2.1,  $\text{CHCl}_3$ ). IR spectrum ( $\nu$ ,  $\text{cm}^{-1}$ ): 1750, 1718, 1695, 1674, 1464, 1379, 1278, 1234, 1212, 1067.  $^1\text{H}$  NMR spectrum ( $\text{CDCl}_3$ ,  $\delta$ , ppm, J/Hz): 0.56 (3H, s, Me-7), 0.85 (3H, d, *J* = 6.9, Me), 0.86 (3H, d, *J* = 6.9, Me), 0.94–1.04 (1H, m,  $\text{H}_{\text{eq}}-10$ ), 1.10 (3H, s, Me-10a), 1.12–1.18 (1H, m,  $\text{H}_{\text{eq}}-9$ ), 1.19–1.25 (1H, m,  $\text{H}_{\text{eq}}-11$ ), 1.27–1.38 (2H, m,  $\text{H}_{\text{eq}}-6$ ,  $\text{H}_{\text{ax}}-10$ ), 1.39–1.49 (2H, m,  $\text{H}_{\text{ax}}-6$ , 9), 1.55 (1H, d, *J* = 12.7,  $\text{H}_{\text{eq}}-8$ ), 1.69–1.78 (1H, m,  $\text{H}_{\text{ax}}-8$ ), 1.78–1.85 (2H, m, H-10b,  $\text{H}_{\text{ax}}-11$ ), 1.94–2.09 (2H, m,  $\text{H}_{\text{eq}}-5$ , H-15), 2.28–2.35 (2H, m,  $\text{H}_{\text{ax}}-5$ , H-6a), 2.83 (1H, br.s, H-12), 3.16 (1H, br.s, H-12a), 3.64 (3H, s, COOMe), 5.44 (1H, s, H-14), 6.45 (1H, d,  $J_{2-3} = 10.2$ , H-2), 6.60 (1H, d,  $J_{3-2} = 10.2$ , H-3).  $^{13}\text{C}$  NMR spectrum ( $\text{CDCl}_3$ ,  $\delta$ , ppm): 15.83 (q, Me), 16.58 (q, Me), 17.01 (t, C-9), 19.98 (q, Me), 20.24 (q, Me), 22.01 (t, C-6), 30.53 (t, C-11), 31.60 (t, C-5), 32.61 (d, C-15), 36.52 (t, C-8), 37.91 (s, C-10a), 38.12 (t, C-10), 40.13 (d, C-12), 45.90 (s, C-4b), 46.29 (d, C-6a), 46.66 (s, C-7), 47.81 (d, C-10b), 52.64 (q, COOMe), 57.05 (d, C-12a), 65.71 (s, C-4a), 127.51 (d, C-14), 138.48 (d, C-3), 143.87 (d, C-2), 148.31 (s, C-13), 170.58 (s, COOMe), 184.95 (s, COO), 194.19 (s, C-4=O), 198.42 (s, C-1=O).

**Procedural Aspects of the Theoretical Calculations.** Theoretical calculations were performed using the Gaussian 09 quantum-chemical program [10]. The DFT–B3LYP method [11–13] with basis set 6-311+G(d,p) [14] was used to optimize the molecular structures (reagents, TS, reaction products) and to solve the vibrational problem. It was shown [15] that results that correlated exactly with the experimental data were obtained with acceptable time constraints if this approach was used to estimate the thermodynamic and activation parameters of the Diels–Alder reaction.

The thermodynamic parameters were calculated for an ideal gas at 298 K and modeled experimental conditions with CH<sub>2</sub>Cl<sub>2</sub> solvent (polarized continuum model [16]) at 295 K.

Quantum-chemical calculations were performed on the supercomputer at the Ufa Inst. Chem., RAS.

## ACKNOWLEDGMENT

The work was sponsored by a Grant of the RF President for Leading Scientific Schools No. NSh-1700.2014.3.

## REFERENCES

1. G. A. Tolstikov, T. G. Tolstikova, E. E. Shul'ts, S. E. Tolstikov, and M. V. Khvostov, *Resinous Acids of Russian Conifers. Chemistry, Pharmacology* [in Russian], Geo, Novosibirsk, 2011, 395 pp.
2. G. F. Vafina, R. R. Fazlyev, F. Z. Galin, and L. V. Spirikhin, *Zh. Org. Khim.*, **45** (4), 515 (2009); G. A. Tolstikov, E. E. Shul'ts, T. Sh. Mukhametyanova, I. P. Baikova, and L. V. Spirikhin, *Zh. Org. Khim.*, **29**, 698 (1993).
3. N. Ardabilchi, J. M. Bruce, and J. Khalafy, *J. Sci. Islamic Repub. Iran*, **11** (3), 195 (2000).
4. B. Kumar, S. M. Suryawanshi, and D. S. Bhakuni, *Tetrahedron Lett.*, **36** (26), 4625 (1995).
5. A. Mukhopadhyay, S. M. Ali, M. Husain, S. N. Suryawanshi, and D. S. Bhakuni, *Tetrahedron Lett.*, **30** (14), 1853 (1989).
6. G.-R. Cai, Z. Guan, and Y.-H. He, *Synth. Commun.*, **41**, 3016 (2011).
7. F. A. Carey and R. J. Sundberg, *Advanced Organic Chemistry. Part B: Reaction and Synthesis*, Kluwer Academic/Plenum Publishers, 2001, 965 pp.
8. M. F. Ansell, B. W. Nash, and D. A. Wilson, *J. Chem. Soc.*, 3012 (1963).
9. N. N. Vorozhtsov and V. P. Mamaev, *Sbornik Statei Obshch. Khim.*, **1**, 533 (1953).
10. M. J. Frisch, G. W. Trucks, H. B. Schlegel, G. E. Scuseria, M. A. Robb, J. R. Cheeseman, G. Scalmani, V. Barone, B. Mennucci, G. A. Petersson, H. Nakatsuji, M. Caricato, X. Li, H. P. Hratchian, A. F. Izmaylov, J. Bloino, G. Zheng, J. L. Sonnenberg, M. Hada, M. Ehara, K. Toyota, R. Fukuda, J. Hasegawa, M. Ishida, T. Nakajima, Y. Honda, O. Kitao, H. Nakai, T. Vreven, J. A. Montgomery, Jr., J. E. Peralta, F. Ogliaro, M. Bearpark, J. J. Heyd, E. Brothers, K. N. Kudin, V. N. Staroverov, T. Keith, R. Kobayashi, J. Normand, K. Raghavachari, A. Rendell, J. C. Burant, S. S. Iyengar, J. Tomasi, M. Cossi, N. Rega, J. M. Millam, M. Klene, J. E. Knox, J. B. Cross, V. Bakken, C. Adamo, J. Jaramillo, R. Gomperts, R. E. Stratmann, O. Yazyev, A. J. Austin, R. Cammi, C. Pomelli, J. W. Ochterski, R. L. Martin, K. Morokuma, V. G. Zakrzewski, G. A. Voth, P. Salvador, J. J. Dannenberg, S. Dapprich, A. D. Daniels, O. Farkas, J. B. Foresman, J. V. Ortiz, J. Cioslowski, and D. J. Fox, *Gaussian 09*, Revision C.01, Gaussian Inc., Wallingford, CT (2010).
11. A. D. Becke, *J. Chem. Phys.*, **98**, 5648 (1993).
12. C. Lee, W. Yang, and R. G. Parr, *Phys. Rev. B*, **37**, 785 (1988).
13. B. Miehlich, A. Savin, H. Stoll, and H. Preuss, *Chem. Phys. Lett.*, **157**, 200 (1989).
14. A. D. McLean and G. S. Chandler, *J. Chem. Phys.*, **72**, 5639 (1980).
15. S. S. Borisevich, I. Tsipisheva, A. V. Kovalskaya, and S. L. Khursan, *J. Theor. Comput. Chem.*, **13** (6), 1450048 (2014); DOI: 10.1142/S0219633614500485
16. J. Tomasi, B. Mennucci, and R. Cammi, *Chem. Rev.*, **105**, 2999 (2005).